



Proteomic and Single-Cell Transcriptomic Dissection of Human Plasmacytoid Dendritic Cell Response to Influenza Virus

Mustafa H. Ghanem^{1,2}, Andrew J. Shih², Houman Khalili², Emily G. Werth³, Jayanta K. Chakrabarty³, Lewis M. Brown³, Kim R. Simpfendorfer^{1,2} and Peter K. Gregersen^{1,2*}

¹ Department of Molecular Medicine, Donald & Barbara Zucker School of Medicine at Hofstra/Northwell, Hempstead, NY, United States, ² The Institute of Molecular Medicine at The Feinstein Institutes for Medical Research, Manhasset, NY, United States, ³ Quantitative Proteomics and Metabolomics Center, Department of Biological Sciences, Columbia University, New York, NY, United States

OPEN ACCESS

Edited by:

Jagadeesh Bayry,
Indian Institute of Technology
Palakkad, India

Reviewed by:

Pärt Peterson,
University of Tartu, Estonia
Yuchun Du,
University of Arkansas, United States

*Correspondence:

Peter K. Gregersen
pgregers@northwell.edu

Specialty section:

This article was submitted to
Molecular Innate Immunity,
a section of the journal
Frontiers in Immunology

Received: 14 November 2021

Accepted: 24 February 2022

Published: 23 March 2022

Citation:

Ghanem MH, Shih AJ, Khalili H, Werth EG, Chakrabarty JK, Brown LM, Simpfendorfer KR and Gregersen PK (2022) Proteomic and Single-Cell Transcriptomic Dissection of Human Plasmacytoid Dendritic Cell Response to Influenza Virus. *Front. Immunol.* 13:814627. doi: 10.3389/fimmu.2022.814627

Plasmacytoid dendritic cells [pDCs] represent a rare innate immune subset uniquely endowed with the capacity to produce substantial amounts of type-I interferons. This function of pDCs is critical for effective antiviral defenses and has been implicated in autoimmunity. While IFN-I and select cytokines have been recognized as pDC secreted products, a comprehensive agnostic profiling of the pDC secretome in response to a physiologic stimulus has not been reported. We applied LC-MS/MS to catalogue the repertoire of proteins secreted by pDCs in the unperturbed condition and in response to challenge with influenza H1N1. We report the identification of a baseline pDC secretome, and the repertoire of virus-induced proteins including most type-I interferons, various cytokines, chemokines and granzyme B. Additionally, using single-cell RNA-seq [scRNA-seq], we perform multidimensional analyses of pDC transcriptional diversity immediately *ex vivo* and following stimulation. Our data evidence preexisting pDC heterogeneity, with subsequent highly specialized roles within the pDC population upon stimulation ranging from dedicated cytokine super-producers to cells with APC-like traits. Dynamic expression of transcription factors and surface markers characterize subclusters within activated pDCs. Integrating the proteomic and transcriptomic datasets confirms the pDC-subcluster origin of the proteins identified in the secretome. Our findings represent the most comprehensive molecular characterization of primary human pDCs at baseline, and in response to influenza virus, reported to date.

Keywords: influenza virus, plasmacytoid DCs, interferon, secretome and transcriptome analysis, single cell RNA seq

INTRODUCTION

pDCs were presumptively identified in 1958 as cells with a ‘plasma cell-like’ morphology observed in human splenic white pulp and lymph nodes (1). Decades later, these cells were isolated from the circulation as the ‘natural IFN-producing cells’ (2). pDCs are notable for their constitutive high expression of the IFN-inducer IRF7 and the nucleic acid sensors TLR7 and TLR9. Together, with

their highly developed endoplasmic reticulum [ER], pDCs are poised to rapidly respond to viral nucleic acid by producing massive amounts of IFN-I. This response is aided by the lack of introns in IFN-I genes, circumventing the steps required for pre-mRNA splicing. Secretion of IFN-I is critical to antiviral defense: signaling downstream of the ubiquitous IFN- α/β receptor results in the induction of antiviral programs, collectively known as the 'interferon signature.' The aberrant activation of the IFN pathway is a hallmark of several autoimmune diseases, as exemplified by systemic lupus erythematosus (3, 4).

Since their initial description, pDCs have mostly been studied in the context of IFN-I production. IFN-I comprises of IFN- α (itself a family of 13 genes encoding 12 distinct polypeptides), IFN- β , IFN- κ , IFN- ω and IFN- ϵ . Traditional approaches have also shown that activated pDCs secrete varying amounts of type-III interferon [IFN-III], TNF- α , IL-6 and CXCL10. Historically, these methods have relied on pDC stimulation with well-characterized synthetic TLR agonists and used analyte-specific ELISAs for readout. To our knowledge, a comprehensive profiling of the primary human pDC secretome in response to a physiologically relevant stimulus has not been reported. Moreover, whether pDCs maintain production of secreted proteins in the baseline 'idle' state has not been explored. Plasma cells, whose morphology bears striking similarity to pDCs, are likewise a rare immune subset, but are notable for their baseline secretion of massive amounts of immunoglobulin necessary for humoral immunity. To address these gaps in knowledge, we catalogued the pDC protein secretome from primary human pDCs using LC-MS/MS for both unstimulated and influenza H1N1 treated conditions. Our data reveal an abundance of known pDC products in addition to novel pDC-sourced protein candidates.

Another characteristic feature of pDCs is their 'diversity' following stimulation. It has long been known that upon stimulation, only a minority of pDCs ultimately produce IFN-I, with the remainder assuming alternative or unrecognized roles (5–7). These studies have been limited by the monoclonal antibodies used in flow cytometry, which cannot capture the breadth of pDC heterogeneity. We therefore endeavored to characterize pDC transcriptional states immediately *ex vivo* as well as following stimulation with influenza H1N1 using scRNA-seq. Our data suggest the presence of preexisting pDC transcriptional variation, and further define clearly specialized cell fates post-stimulation.

RESULTS

pDC Secretome Profiling by LC-MS/MS

A major challenge to proteomic profiling of serum or culture media is the phenomenon of ionization suppression, whereby species dominant in a solution (such as albumin and immunoglobulin in serum) compete for ionization energy with less abundant species thereby impeding their detection (8). To minimize the necessary media protein supplement, we tested a variety of culture conditions assaying for pDC viability and IFN-I

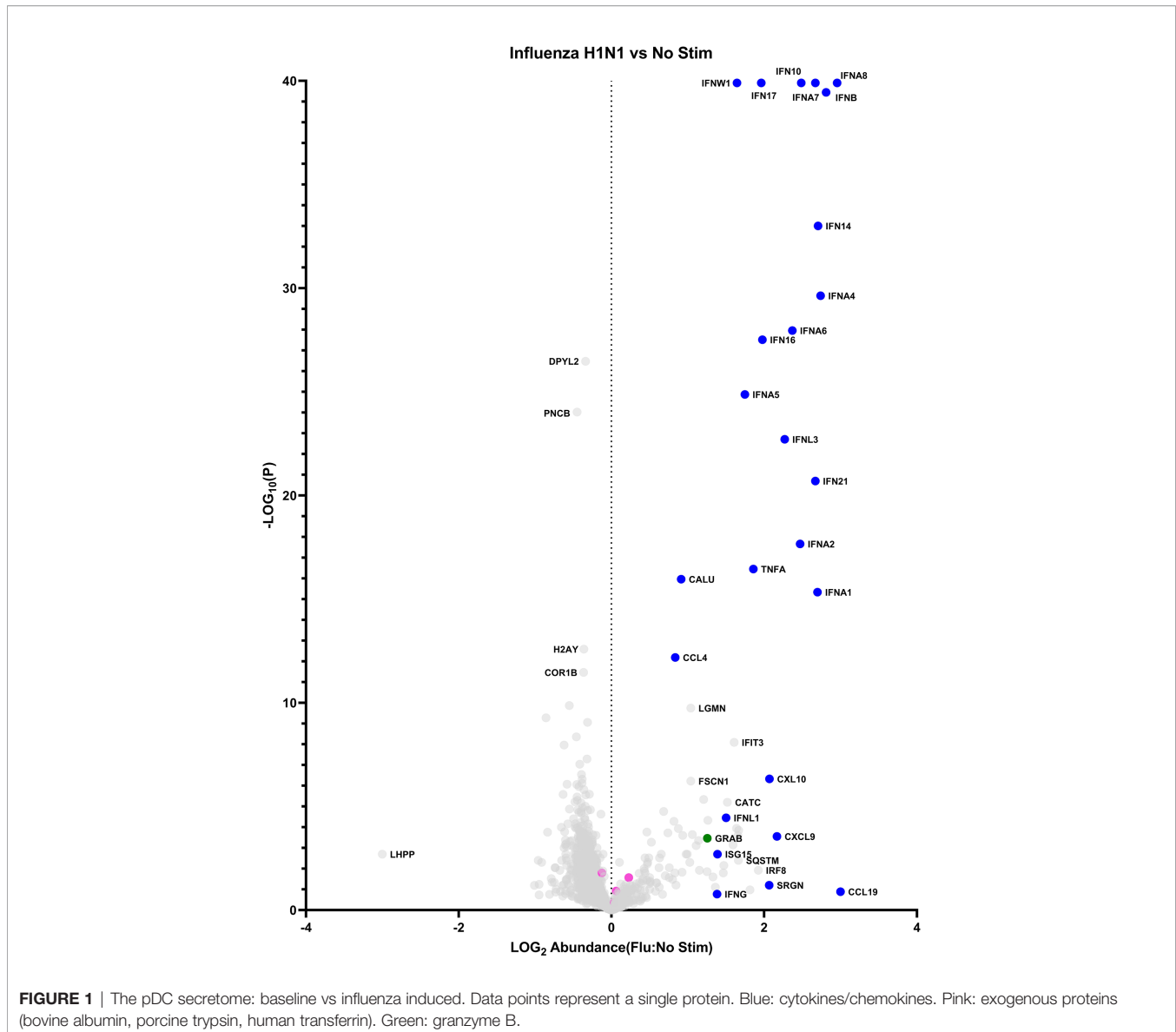
output as a measure of media compatibility. pDCs remained viable and produced significant quantities of IFN- α with fetal calf serum (FCS) levels down to 1%. However, we observed that even trace amounts of FCS accounted for the majority of media protein following pDC culture. Therefore, we opted to use serum-free media supplemented with minimal amounts of albumin, insulin and holo-transferrin. pDCs maintained IFN-I production capacity and viability in this media similar to media containing FCS (**Figure S1**). Media completely free of exogenous protein was incompatible with pDC interferon production (data not shown).

pDCs were enriched from three female donors. In order to maximize pDC recovery, pDC yield was prioritized over pDC purity (**Figure S2**). Cells were cultured at high density for 24 hours in the presence or absence of influenza H1N1 (A/PR/8/34). Following stimulation, cells were collected for viability assessment, culture media was cleared of cellular debris and media protein was precipitated for proteomic processing by LC-MS/MS. As has been previously established, pDC viability is enhanced *ex vivo* with stimulation (9). Roughly 94% of the detected peptides corresponded to the exogenous media additives BSA, human transferrin and porcine trypsin (used in proteomic processing), reinforcing the imperative to minimize non-pDC derived media proteins *a priori* (**Figure S3A**). The remainder of peptides were attributable to the cultured cells, identifying a total of 1,241 protein species, 819 of which were identified with high confidence, represented by 2 or more peptides (**Figures S3B, C**). A list of identified proteins can be found in the supplementary appendix (**Table S1, Data Sheet 2**).

Detected proteins which did not differ in abundance between stimulated and unstimulated conditions generally include exogenous media additives and human serum proteins not known to be produced by hematopoietic cells (**Figure S4A**). The latter likely represent human serum proteins carried over through pDC isolation from whole blood. The protein secretome of unstimulated pDCs was enriched for proteins not known to be secreted, including proteins with various roles in the cytoskeleton and cellular metabolism (**Figure S4B**). These proteins likely represent leakage from dying cells, and is consistent with the observed relative impairment of pDC viability in culture in the absence of stimulation.

Several proteins were present in a manner consistent with baseline secretory function of pDCs, however. These include pigment epithelium-derived factor/*SERPINF1*, alpha 2-antiplasmin/*SERPINF2*, and prostaglandin D2 synthase/*PTGDS*. These proteins are annotated as 'secreted' in the UniProt database and are recognized as enriched for expression in pDCs among circulating leukocytes in the Human Protein Atlas (<http://www.proteinatlas.org/>) (10). IL-16 is also enriched in the unstimulated condition; however, this cytokine is expressed by numerous cell types and thus may represent a contribution from contaminating non-pDC leukocytes in our cultures.

Stimulation with influenza virus is noted to induce the robust upregulation of numerous cytokines, including all 12 members of the IFN- α protein family (**Figure 1** and **Figures S4C, D**).



Other detected IFN-I members include IFN- β and IFN- ω . IFN- κ and IFN- ϵ were not detected. The IFN-III family was represented by IFN- λ 1 and IFN- λ 3. The sole IFN-II candidate, IFN- γ was observed at low levels and is likely derived from contaminating cells, since this cytokine is not known to be produced by pDCs (see below scRNA-seq data for follow up). Other strongly induced cytokines include TNF- α and IL-6, and the chemokines CXCL9, CXCL10, CCL4 and CCL19. Several proteins encoded by secreted interferon-stimulated genes [ISGs] were detected, including ISG15 and SRGN. Notably, a number of proteins lacking a signal peptide and not annotated as ‘secreted’ elsewhere were overrepresented in the influenza stimulated group, including the proteases cathepsin c, cathepsin z, legumain, and the transcription factor IRF8. Finally, granzyme B is released from pDCs in response to influenza virus. Metrics supporting the identification of select proteins of interest are presented in **Table 1**.

These data confirm IFN- α as the chief secreted product of stimulated pDCs. Moreover, they represent a more comprehensive and agnostic analysis of non-interferon secreted products, both upon stimulation, and in the unperturbed condition.

pDC Diversification in Response to Influenza Virus Mapped by scRNA-Seq

Our above data are consistent with the well-established robust IFN- α secretion capabilities of pDCs. In our hands, we calculated the 24hr IFN- α production capacity of pDCs to 4.5-7pg/cell when averaged over a population of pure pDCs (**Figure S5**). Making this value more astonishing is the reported observation that upon stimulation, only a minor fraction of pDCs stain positive for IFN- α when assayed by flow cytometry. This observation is limited by the fact that anti-IFN- α mAbs can only detect one to several of the IFN- α subtypes at a time, leaving

TABLE 1 | Supporting protein identification evidence for example differently expressed proteins from **Figure 1**, the pDC secretome: baseline vs influenza induced*.

UniProt ID	Protein	Mascot Peptide Count	PD # Unique Peptides	Mascot Protein Score	Mascot Ion Score	Mascot Homology Threshold	PD % Coverage	PD # PSM	Ratio (Flu stim/NO STIM)	P-value (Flu stim vs. NO STIM)
CATC_HUMAN	Dipeptidyl peptidase 1	14	15	719	62	16	41.3	22	33.0	6.3E-06
COR1B_HUMAN	Coronin-1B	5	3	144	45	17	6.2	3	0.4	3.4E-12
CXCL9_HUMAN	C-X-C motif chemokine 9	8	5	304	56	17	42.1	7	147.1	2.8E-04
CXL10_HUMAN	C-X-C motif chemokine 10	6	6	318	56	17	47.6	10	117.7	4.7E-07
DPYL2_HUMAN	Dihydropyrimidinase-related protein 2	21	21	1065	61	17	55.4	25	0.5	3.4E-27
FSCN1_HUMAN	Fascin	12	10	405	47	17	25.6	12	11.0	6.1E-07
GRAB_HUMAN	Granzyme B	2	6	107	41	16	20.0	6	18.1	3.4E-04
H2AY_HUMAN	Core histone macro-H2A.1	12	10	369	56	18	37.2	12	0.4	2.6E-13
IFIT3_HUMAN	Interferon-induced protein with tetratricopeptide repeats 3	7	6	249	45	16	19.7	8	40.5	8.1E-09
IFN10_HUMAN	Interferon alpha-10	2	3	427	60	16	27.7	22	306.2	0
IFN14_HUMAN	Interferon alpha-14	4	4	837	46	16	46.6	42	508.0	1.0E-33
IFN16_HUMAN	Interferon alpha-16	6	5	789	61	17	46.6	24	94.9	3.1E-28
IFN17_HUMAN	Interferon alpha-17	2	2	696	68	17	47.4	33	91.6	0
IFN21_HUMAN	Interferon alpha-21	7	1	1432	64	17	52.6	59	468.2	2.0E-21
IFNA1_HUMAN	Interferon alpha-1/13	10	10	947	52	18	51.5	47	499.3	4.6E-16
IFNA2_HUMAN	Interferon alpha-2	4	4	533	59	18	36.2	20	296.3	2.2E-18
IFNA4_HUMAN	Interferon alpha-4	4	2	607	50	16	36.0	31	549.7	2.3E-30
IFNA5_HUMAN	Interferon alpha-5	2	2	1333	56	21	46.6	58	56.1	1.3E-25
IFNA6_HUMAN	Interferon alpha-6	5	5	361	28	16	38.1	26	233.7	1.1E-28
IFNA7_HUMAN	Interferon alpha-7	10	3	390	35	15	45.5	27	469.5	0
IFNA8_HUMAN	Interferon alpha-8	4	7	947	41	17	46.9	48	901.5	0
IFNB_HUMAN	Interferon beta	3	7	93	33	17	27.8	7	647.0	3.6E-40
IFNL1_HUMAN	Interferon lambda-1	3	4	151	34	18	26.8	6	31.7	3.5E-05
IFNL3_HUMAN	Interferon lambda-3	2	3	222	42	18	36.4	6	186.3	2.0E-23
IFNW1_HUMAN	Interferon omega-1	3	8	182	30	16	26.2	16	44.2	0
ISG15_HUMAN	Ubiquitin-like protein ISG15	5	4	218	49	17	26.9	5	24.5	2.0E-03
LGMN_HUMAN	Legumain	4	3	135	56	17	13.4	3	11.0	1.8E-10
PNCB_HUMAN	Nicotinate phosphoribosyltransferase	4	3	89	35	17	8.1	3	0.4	9.5E-25
SQSTM_HUMAN	Sequestosome-1	1	3	74	50	16	11.0	3	46.0	4.0E-03
TNFA_HUMAN	Tumor necrosis factor	5	6	137	38	16	37.8	8	72.1	3.5E-17

*Data generated by Mascot server V. 2.5.1., Proteome Discoverer v. 1.4 (for protein identification), or Elucidator V. 4.0.0.2.31 (for differential expression).

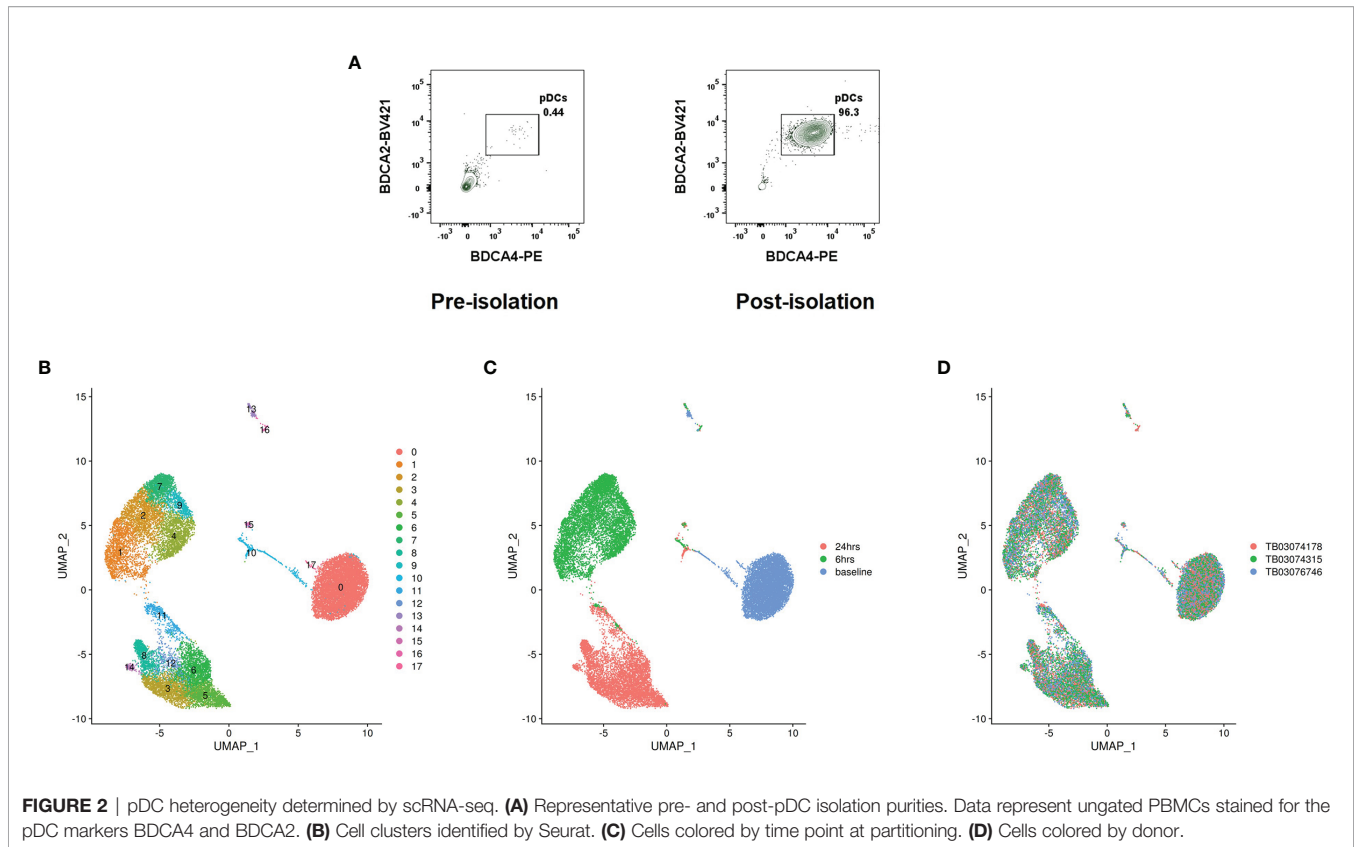
open the possibility that while some pDCs stain positive for IFN- α , others account for the production of the uncaptured subtypes. Nevertheless, these reported findings suggest that what is traditionally thought of as a homogenous pool of pDCs may diverge in function following stimulation. pDC heterogeneity pre- and post-stimulation has been described (see *Discussion* below). These studies were similarly limited, however, by the selection of mAbs used to delineate the pDC subpopulations. Therefore, we undertook a *de novo* characterization of pDC diversity, at baseline and in response to influenza virus using scRNA-seq.

pDCs were isolated from three genotyped female donors to near total purity (**Figure 2A**). A third of pDCs from each donor was immediately partitioned for baseline pDC transcriptional profiling. The remainder were cultured with influenza virus for 6 and 24hrs; with cells partitioned at the close of each time point. To avoid batch effects, cells from the different donors were pooled upon partitioning by time point (*ex vivo*, 6hrs/flu, 24hrs/flu), with subsequent library preparation and Illumina sequencing steps shared among donors. Cell yields and sequencing output are reflected in **Table S2**. Single cells were

assigned to their respective donors using Demuxlet (11). Donor-specific signals were controlled using Harmony (12). Clusters were generated using Seurat (13) (**Figure 2B**). The data reveal that the cells segregate predominantly by time point (**Figure 2C**), with clusters evident within each major condition. Coloring cells by donor reveals that the donor cells are well-interspersed among the clusters (**Figure 2D**), negating the possibility that donor-specific characteristics are main drivers of cell diversity. 18 clusters are identified by Seurat. The top differentiating genes among the clusters are listed in the supplementary appendix (**Table S3**).

Of the clusters, clusters 13 and 16 represent minor B and T cell contamination of the pDC cultures, respectively. Cluster 17 represents AXL⁺ pDCs, a recently described dendritic cell with an intermediate phenotype between pDCs and cDCs (14). The remaining clusters represent bona fide pDCs with distinct transcriptional profiles.

Clusters 1 and 11, in the 6hr and 24hr influenza virus-treated conditions, respectively, represent the IFN producing cells (**Figure 3A**). These clusters mapped with close proximity to each other across the two time points. Notably, these clusters



expressed the totality of IFN-alpha genes and other IFN-Is produced by pDCs (**Figure 3B**). TCF4, the transcription factor instructing pDC identity, is depleted in these clusters, whereas ID2, the transcription factor opposing pDC identity, is upregulated (see next paragraph). Moreover, the classical pDC markers NRP1, CLEC4C and CD123 are depleted in the IFN producing cells (**Figure 4A**). These data confirm that among a population of pDCs treated with the same stimulus, only a minor portion mature into the IFN producing population. These cells appear to adopt a dedicated role, losing canonical transcriptional features of pDCs. Alternative surface markers suggested by the data for the IFN producers include IL18RAP, LILRA5 and LILRB2, among others (**Figure 4B**).

Another notable phenomenon within the single cell data was the dynamism of expression of the transcription factors TCF4 and ID2. (**Figure 5A**). TCF4 dictates pDC identity (15), and its continuous expression is required for the maintenance of this identity (16). ID2 is an antagonist of TCF4 which instructs a cDC profile. All pDCs *ex vivo* were TCF4⁺ID2⁻, whereas upon stimulation, expression of these transcription factors varied widely by cluster. Cluster 5 is particularly prominent for loss of TCF4 and gain of ID2. This change is accompanied by upregulation of the T cell co-stimulatory markers CD80/CD86, cDC markers FSCN1, and the secondary lymphoid organ T cell zone homing receptor CCR7 (**Figure 5B**). These observations suggest that cluster 5 is a cDC/APC-like derivative of pDCs whose principal role is in antigen presentation to T cells.

Cluster 8 represents a group of cells retaining classical pDC features even following 24hr culture with influenza virus. These markers include CLEC4C and CD123, as well as pDC specific genes such as SCAMP5, GZMB, TCF4 and IRF7 (**Figure S6**). Whether this cluster represents a group of cells resistant to stimulation, or a 'return to baseline' phenotype, remains to be determined.

Finally, pDC heterogeneity is evident at baseline (**Figure 6**). On fine grain clustering, 9 subclusters are identified within the unstimulated group partitioned immediately *ex vivo*. Importantly, the classical pDC markers NRP1 and CLEC4C are evenly distributed among these clusters, as is the master pDC regulator TCF4. ID2 is absent. PTGDS, TCL1A, TCL1B and IGLC2 clearly distinguish these clusters. Whether this preexisting heterogeneity informs maturation into IFN producers or other phenotypes following stimulation is the subject of future investigations. Taken together, this dataset represents a multidimensional, discovery-led approach revealing pDC transcriptional diversity at baseline and further upon stimulation with influenza virus.

Integration of LC-MS/MS and scRNA-Seq Datasets

The scRNA-seq data also allow for a more complete understanding of the secretome data discussed previously. As mentioned, pDCs in latter experiments were only ~60% pure, versus near total purity in the scRNA-seq dataset. Many

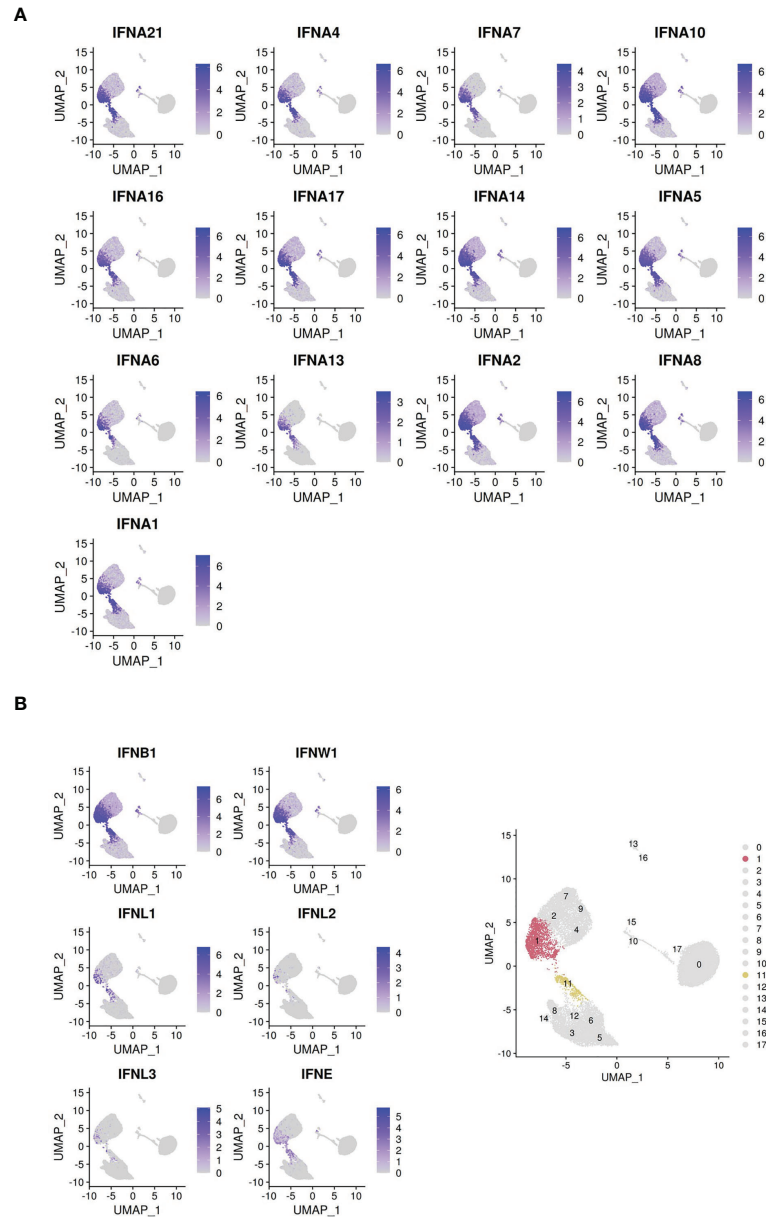


FIGURE 3 | Clusters colored by IFN-I gene expression. **(A)** Cells colored by IFN- α subtype gene expression. **(B)** Cells colored by non-IFN- α type I interferon gene expression. Bottom right panel: highlight of clusters 1 and 11 identified by Seurat.

identified cytokines, such as IFN-I and IFN-III, are readily attributable to pDCs. Other identified cytokines and chemokines, such as IL-16, CXCL9, CCL4 and CCL9 may or may not be pDC-derived. As the secretome and scRNA-seq experiments similarly involved pDC stimulation with influenza virus over a course of 24hrs, the scRNA-seq data may be leveraged to determine whether pDCs are in fact contributing the identified proteins in the secretome dataset. As shown in **Figure 7**, IL-16, CCL4 and CXCL10 are confirmed to be pDC-derived, whereas IFNG is confirmed to come from non-pDCs. Interestingly, IL16 is expressed predominantly among cells of the

ex vivo time point, and is lost upon stimulation, confirming its status as a member of the ‘baseline’ pDC secretome discussed above.

In Vitro Validation of pDC Markers Suggested by scRNA-Seq

The above findings merit validation and further exploration in the appropriate experimental and clinical contexts. For example, the finding that IFN- α ⁺ pDCs gain a novel surface marker profile can be validated by flow cytometry. LILRB2 is noted to be enriched for expression in the IFN- α producers. Gating on the

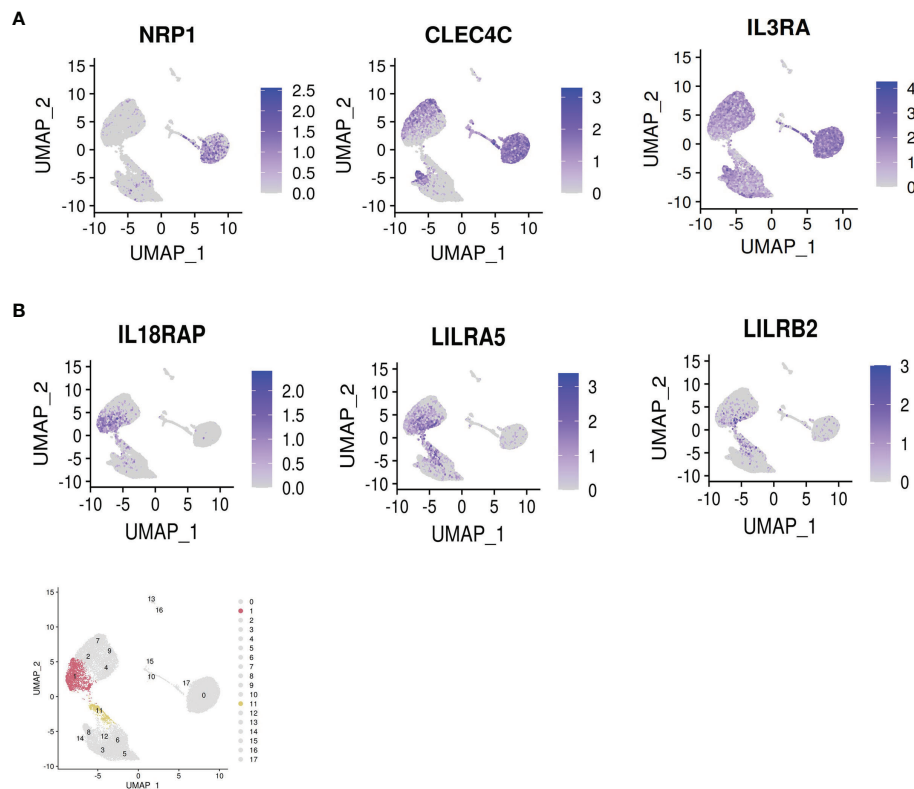


FIGURE 4 | Dropout of classical pDC markers and appearance of novel surface markers on the IFN- α^+ cells. **(A)** Dropout of the classical pDC surface antigens NRP1 [BDCA4], CLEC4C [BDCA2] and IL3RA [CD123] in the IFN-producers. **(B)** Novel suggested surface markers in the IFN-producers. Bottom panel: highlight of clusters 1 and 11 identified by Seurat.

IFN- α^+ cells in a population of pDCs stimulated with influenza virus demonstrates significant surface staining for LILRB2 relative to the IFN- α^- cells (**Figure 8A**). Similarly, other clusters can be further explored. Cluster 5, shown to adopt a ‘cDC-like’ transcriptional profile, is noted to upregulate expression of CD80, CD86, and CCR7. Cells of this cluster can be detected using mAbs against these respective markers after overnight culture with influenza virus, whereas cells cultured in the absence of virus do not stain for any of these markers (**Figure 8B**). Future validation in samples from patients with SLE, influenza or COVID-19 will be necessary to follow up on the clinical relevance of these data.

DISCUSSION

pDC Secretory Activity

pDCs were definitively identified as the ‘natural-IFN producing cell’ in the circulation, and IFN-I has been the principle focus of pDC investigations since. Besides IFN-I, traditional approaches have shown that pDCs also produce substantial amounts of IFN-III, TNF-alpha, IL-6 and CXCL10, typically using single-analyte ELISAs and often in response to synthetic stimuli. An early attempt by Decalf et al. towards characterizing the pDC secretome utilized a 12-plex Luminex assay to show that pDCs also produce CCL2,

CCL3, CCL4, CCL5, IL-1RA and IL-8 in response to stimulation with influenza virus or ODN-2216 (17). Another group attempted to characterize DC secretion *via* 2D-PAGE followed by shotgun proteomics from monocyte-differentiated DCs (18). The resemblance of *in vitro* differentiated DCs to primary DCs is questionable, however, as even the most advanced techniques produce cells transcriptionally distant from their natural counterparts (Martin Jakobsen, personal communication).

To our knowledge, a comprehensive and agnostic study of the pDC secretome has not been previously attempted. Moreover, secreted products of unperturbed pDCs have not been systematically catalogued. To accomplish these goals, we subjected media protein preparations from high density pDC cultures to LC-MS/MS analysis. To increase the odds of detecting pDC-derived proteins, we used the minimal amount of exogenous protein possible. In addition, we did not enrich the pDCs to total purity, as this would inevitably reduce the yield of pDCs. The finding that bovine albumin was the dominant species in the culture media was expected, the extent of which corroborated the need to minimize the presence of media protein additive. Methods exist to deplete albumin from sample preparations; we elected not to use these methods for risk of introducing identification bias (BSA depletion may also deplete non-specifically).

We performed a pilot secretome analysis on unstimulated and ODN-2216 stimulated pDCs from 3 donors, identifying 293

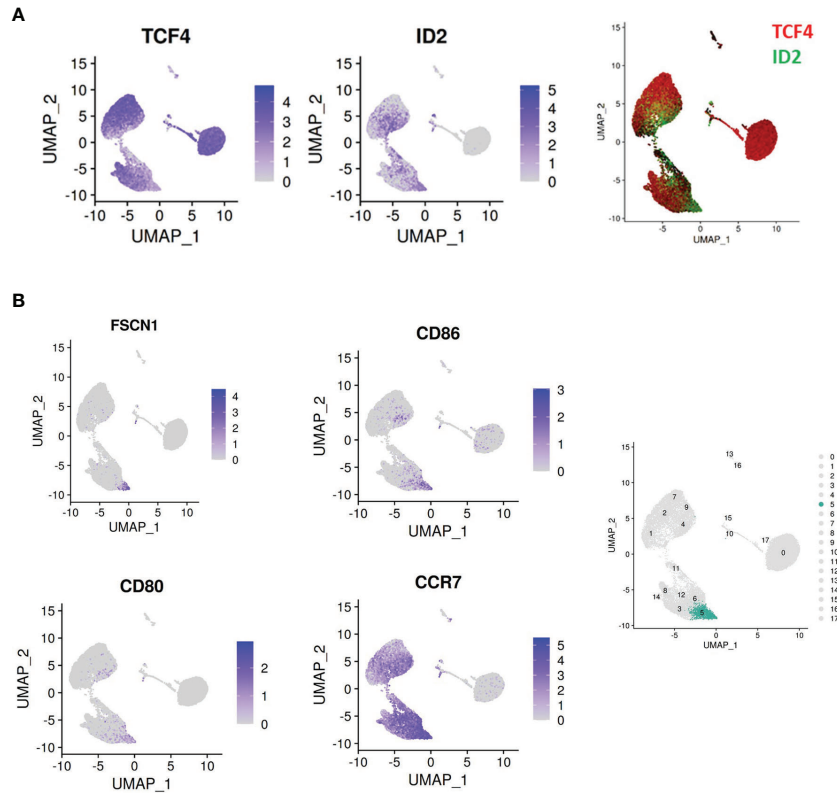


FIGURE 5 | Dynamic regulation of master transcription factors across pDC clusters. **(A)** An inverse relationship is observed between the pDC master regulator TCF4 and the TCF4 antagonist ID2. The cluster 1/11 isthmus is notable for loss of TCF4 and gain of ID2. **(B)** Cluster 5 (highlighted in the right panel) is notable for upregulation of ID2, and the cDC/APC markers CD86, CD80, FSCN1 and CCR7.

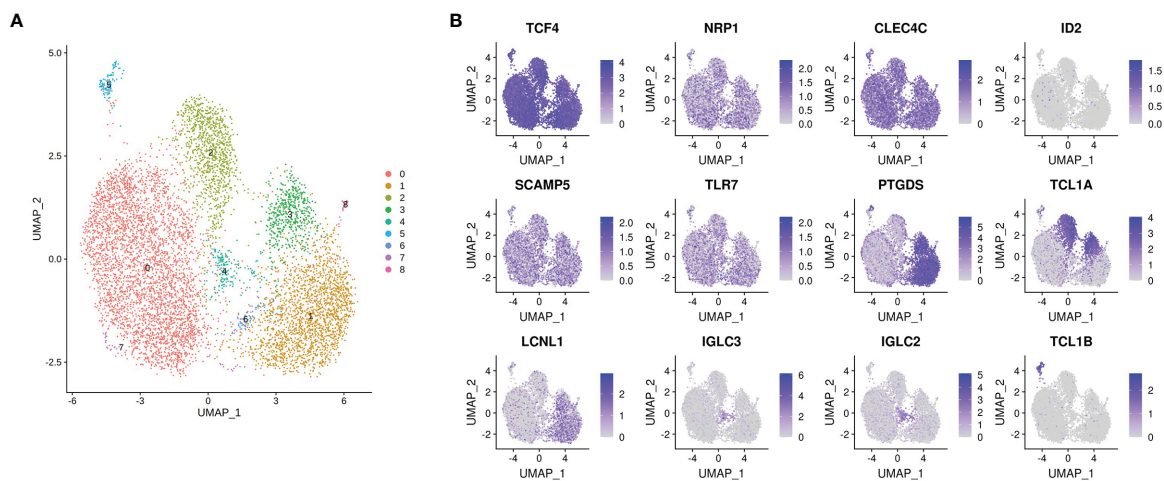


FIGURE 6 | pDC heterogeneity at baseline. **(A)** Cluster 0 (as identified in **Figure 2B**) is further divided into 9 subclusters by Seurat, highlighting preexisting pDC heterogeneity as the cells are isolated *ex vivo*. **(B)** TCF4, NRP1 and CLEC4C are evenly distributed within these subclusters, as expected. ID2 is absent. pDC enriched genes SCAMP5 and TLR7 are also uniformly expressed, whereas PTGDS, TCL1A, LCLN1, IGLC3, IGLC2 and TCL1B distinguish various subclusters.

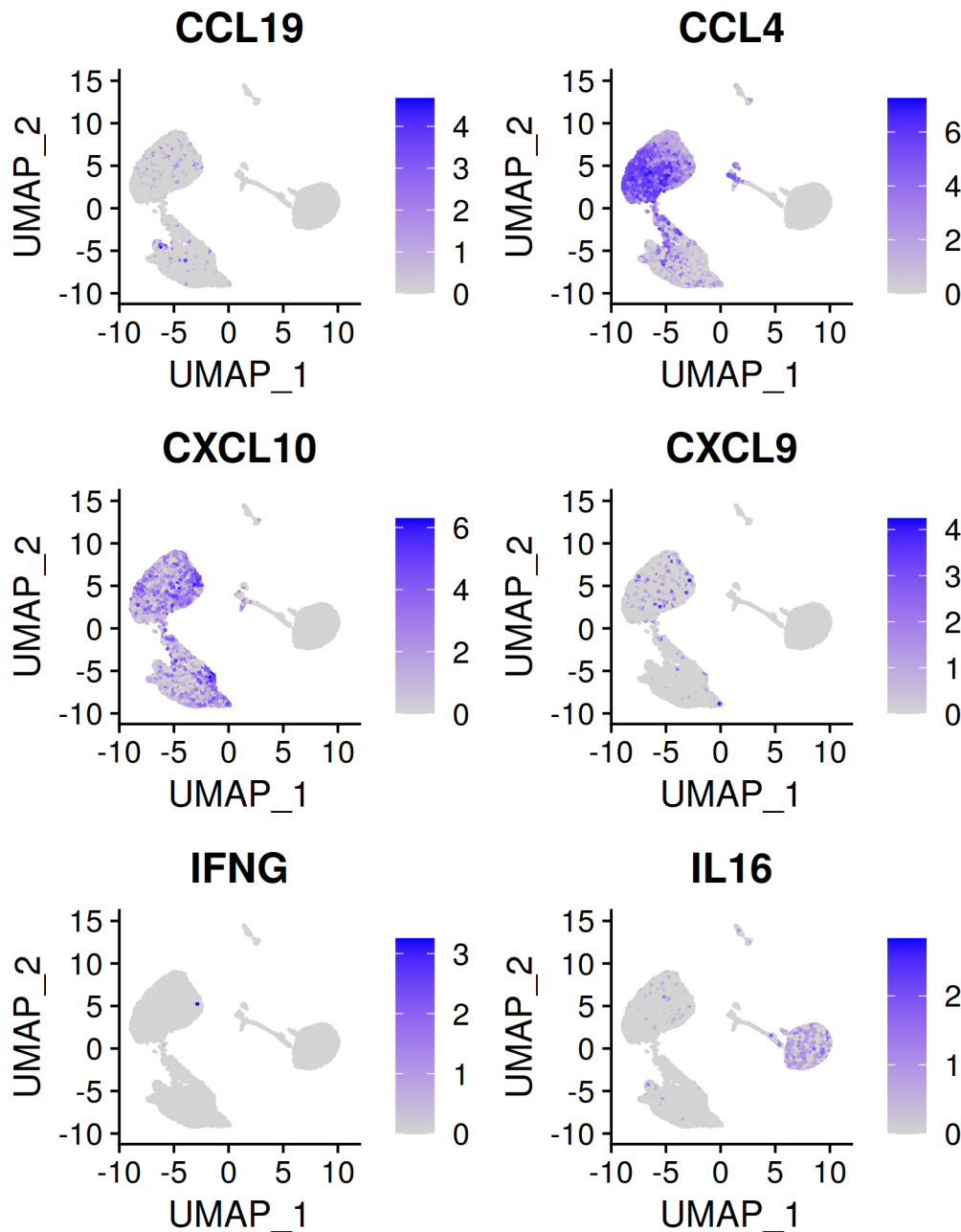


FIGURE 7 | Cytokines/chemokines identified by LC-MS/MS and corresponding transcript presence in the scRNA-seq dataset. CXCL10 is a known pDC chemokine and is upregulated in pDCs upon flu virus treatment. CCL4 can be attributed to pDCs on the basis of upregulation with flu virus seen here. IFNG is not known to be a pDC cytokine, the absence of IFNG in the scRNA-seq dataset confirms the non-pDC origin of this cytokine in the secretome experiment. IL-16 is identified in the secretome data as enriched in the unstimulated condition. This finding is supported by the observation that *ex vivo* pDCs express IL16, whereas flu virus treated pDCs do not.

proteins (data not shown), serving as proof-of-concept. Our follow-up analysis, presented here, using unstimulated and influenza virus-stimulated pDCs from an additional 3 donors netted 1,241 protein identifications. Our approach to analyzing the list of identified proteins prioritized species annotated as ‘secreted’ in the Uniprot database. To ascribe pDCs as the source of a particular protein in the unstimulated condition, we referred

to the Human Protein Atlas to determine the degree of pDC-specific expression. Secreted proteins identified in the influenza virus-treated conditions were ascribed to pDCs on the basis of historical association or upregulation in the scRNA-seq data, which also used influenza virus as the stimulus.

Here, our results suggested the presence of a ‘baseline’ pDC secretome. Interleukin-16 (IL-16/*IL16*), pigment epithelium-

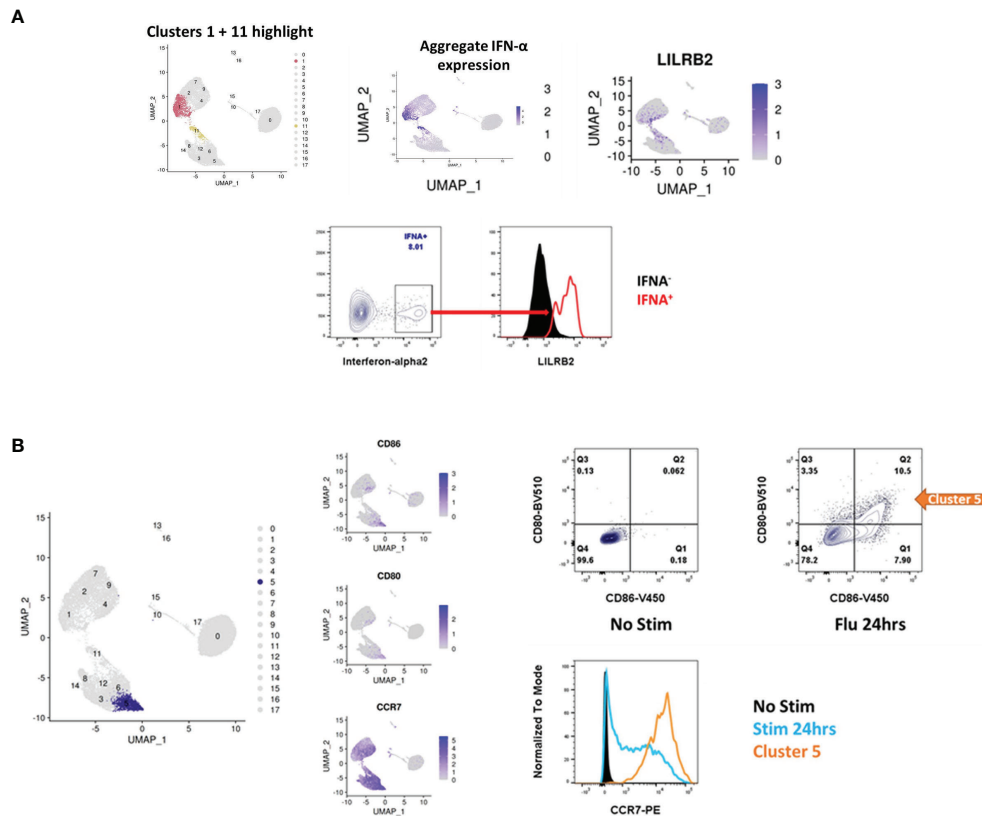


FIGURE 8 | Validation of surface markers suggested by scRNA-seq. **(A)** pDCs in the IFN- α^+ cluster lose canonical pDC markers and adopt new ones (see also, **Figure 4**), including IL18RAP, LILRA5 and LILRB2. Upon stimulation with influenza virus, the population of IFN- α^+ cells stains positive for LILRB2 whereas IFN- α^- cells are negative for LILRB2. **(B)** Cluster 5 is notable for the adoption of a cDC like state, including upregulation of ID2 (**Figure 5**), CD80, CD86 and CCR7. Stimulation of pDCs with influenza virus produces a population of cells which stain for CD80 and CD86, these cells also upregulate expression of CCR7 at the protein level as determined by flow cytometry.

derived factor (PEDF/SERPINF1), alpha-2-antiplasmin (A2AP/SERPINF2) and prostaglandin-D2-synthase (PGD2/PTGDS) are identified as top candidates for pDC-specific secreted proteins in unperturbed conditions. The biological significance of PEDF and A2AP secretion by pDCs has not been explored. PGD2 catalyzes the formation of the arachidonic acid metabolite prostaglandin D2, a neuromodulator and potent vasodilator. A single report (19) described pDCs as a hematopoietic source of PGD2 but does not further examine the role of PGD2 from these cells in particular (19). Other baseline pDC secreted products were also identified, including several additional members of the SERPIN family, although pDCs are likely not the sole source of these proteins among leukocytes. For example, IL-16, a T cell chemoattractant, was identified in the secretome data as enriched in the unstimulated condition. Our scRNA-seq data points to expression of IL-16 in *ex vivo* pDCs which is lost upon stimulation. The Protein Atlas suggests that non-pDCs serve as IL-16 producers as well. Together, these proteins represent underexplored baseline pDC secretory activity.

In the induced secretome, IFN-I was clearly the dominant category of secreted protein, including all 12 IFN- α subtypes, IFN- β and IFN- ω . The IFN-III category was represented *via*

IFN- λ 2 and λ 3. TNF- α , IL-6 and CXCL10—known pDC cytokines, were also well represented. Cytokines less commonly associated with pDCs, such as CCL4 and IFN-gamma, were respectively ruled-in and ruled-out as pDC-sourced on the basis of scRNA-seq data. Not all cytokines reported by Decalf et al. were identified, however. CCL3 and CCL5, for example, were absent in the secretome dataset, but highly upregulated in the IFN-producers in the scRNA-seq dataset. This likely indicates that our secretome analysis missed important identifications, reflecting a technical limitation as currently performed. On the other hand, the cytokines CCL2 and IL-1RA were absent in both secretome and scRNA-seq datasets, suggesting non-pDC contamination as the source of these proteins in Decalf et al.

Granzymes are conventionally thought of in terms of cytotoxic lymphocyte degranulation and represent a major antiviral tool of adaptive immunity (20). The Protein Atlas illustrates preferential expression of granzymes A, H, K and M in CD8 T cells and NK cells, as expected. Granzyme B, however, is by far most highly expressed in pDCs (**Figure S7**). Granzyme B is enriched in the culture media of influenza stimulated pDCs, as observed in the secretome analysis. In the scRNA-seq dataset, GZMB expression is noted at baseline and was lost upon

stimulation, counter to the protein level observation. This finding is consistent with granzyme release *via* fusion of preformed granules with the plasma membrane, a process distinct from IFN secretion, which is induced *de novo* at the transcript level for transit through the secretory pathway.

Overall, the induced pDC secretome confirms the robust reactionary nature of these cells, whose chief product is IFN- α , and argues against baseline hypersecretory function akin to the namesake plasma cells. Other secreted protein products represent a more diverse picture of virus-induced pDC activity. A striking component of the induced secretome consisted of proteins not annotated as secreted yet which are pDC-specific, including IRF8, legumain and various cathepsins. Leakage from dying cells is unlikely to explain the enrichment of these proteins in the media of stimulated cells, as stimulation enhances pDC survival *in vitro*. We hypothesize that pDC stimulation results not only in secretion through the classical ER-Golgi pathway, but also results in the release of protein-loaded exosomes. These exosomes may serve as an alternative method for transferring antiviral programs to recipient cells. Recently it was demonstrated that pDCs form ‘interferogenic synapses’ with viral infected cells (21). Communication of an antiviral program *via* transcription factor and protease loaded exosomes in a paracrine fashion is an exciting avenue for future exploration. This work marks the first agnostic description of the primary human pDC secretome, at baseline, and in response to a physiologic stimulus. Our data support multiple mechanisms of regulated protein release from pDCs, including the classical secretory pathway, degranulation and, putatively, exosome formation.

Transcriptional Diversity of pDCs

pDC heterogeneity pre- and post-stimulation has been described. A CD2^{hi}Lysozyme⁺ population of pDCs was reported to possess enhanced T cell activation properties (22). A similar report describes CD2^{hi}CD5⁺CD81⁺ pDCs as potent inducers of T cell proliferation (23). That a minority of pDCs produce IFN- α upon stimulation has long been known. The evidence for this, however, typically involves intracellular antibody staining for IFN- α towards flow cytometric analyses. As there are 12 IFN- α subtypes, no single IFN- α antibody could detect all subtypes simultaneously. As such, it remained possible that a minority of pDCs produced particular subtypes of IFN- α , with other pDCs producing the remaining subtypes. Alculumbre et al. report a detailed analysis of pDC diversification following stimulation with influenza virus (24). Their results show that upon treatment with influenza virus, pDCs diversify along a 2-parameter, CD80/PDL1 axis. CD80⁺PD-L1⁻ cells adopt APC-like functions with dendritic morphology, whereas CD80⁺PD-L1⁺ cells secrete interferon and retain plasmacytoid morphology. These results were later recapitulated using SARS-CoV-2 as the stimulus (25). Using mass cytometry, it was further shown that human pDCs mount distinct, heterogenous responses dependent on the stimulus (26).

To better understand pDC diversity pre- and post-stimulation in a highly multidimensional format, we analyzed

the transcriptomes of pDCs from 3 donors immediately *ex vivo*, upon 6hrs of influenza virus stimulation and upon 24hrs of influenza virus stimulation at the single-cell level. To our knowledge, we are the first to demonstrate that a single population of IFN-producers is responsible not only for the totality of IFN- α production, but for the other IFN-I family members, IFN-III, and the majority of induced cytokines as well. This population represents roughly 24% of cells at the 6hr time point and 5.5% of cells at the 24hr time point. These clusters are notable for dropout of classical pDC markers, including BDCA4, BDCA2, CD123 and ILT7. pDCs have been reported to diminish in the circulation of SLE patients with active disease (27, 28), patients affected by pandemic influenza (29, 30), and in patients with severe COVID-19 (29–31). This has commonly been interpreted to indicate that pDCs in these patients infiltrate affected tissues, decreasing their presence in the circulation. pDCs have been shown to diminish from the bronchoalveolar fluid of COVID-19 patients (32), however, challenging this theory. Our findings suggest an alternative explanation: pDCs appear to be reduced in these conditions because they are no longer detectable using the standard pDC surface antigens. We suggest alternative surface markers for the detection of IFN-producing, activated pDCs. These markers can then be applied to characterize pDCs in the relevant clinical contexts.

Another notable phenomenon within the single cell data was the dynamism of TCF4/ID2 expression. TCF4 dictates pDC identity (15), and its continuous expression is required for the maintenance of this identity (16). ID2 is an antagonist of TCF4 which instructs a cDC profile. All pDCs *ex vivo* were TCF4⁺ID2⁻, whereas upon stimulation, expression of these transcription factors varied widely by cluster. Cluster 5 is particularly prominent for loss of TCF4 and gain of ID2. This change is accompanied by upregulation of the T cell co-stimulatory markers CD80/CD86, cDC marker FSCN1 and the secondary lymphoid organ T cell zone homing receptor CCR7. These observations suggest that cluster 5 is a cDC/APC like derivative of pDCs whose principal role is in antigen presentation to T cells. A small population, cluster 8, is observed to maintain the panel of pDC specifying transcription factors, including TCF4, SPIB, and IRF8, along with pDC-typical genes including IRF7, GZMB, SCAMP5 and pDC surface markers BDCA2, ILT7 and CD123. Whether the presence of this cluster at 24hrs represents cells unaffected by stimulation or cells which lost and subsequently recovered pDC identity is not clear. It is apparent, nonetheless, that pDC identity reflects a continuous rebalancing of master regulators.

Preexisting heterogeneity is also evident from our data, with 9 baseline subclusters identified. Whether this heterogeneity determines the fate of a particular cell upon influenza virus stimulation remains to be determined. Unfortunately, the genes discriminating these clusters are not expressed at the cell surface, precluding the sorting of live cells towards fate-determination assays. Notably, CD2, CD5 and CD81, markers previously reported to define baseline pDC heterogeneity, did not discriminate these baseline pDC clusters. Rather, these markers were enriched in cluster 17, AXL⁺ pDCs. This population was

recently identified as cells with an intermediate phenotype between pDCs and cDCs (14), and likely explains the enhanced T cell proliferation capacity of the cells reported earlier (22, 23).

A potential limitation of our study in comparing the baseline versus stimulated cells was the exposure of the stimulated cells to culture media. While this may partially explain the clustering distance between the baseline cells and stimulated cells, we believe that the dramatic upregulation of many genes in the stimulated cells can be more specifically explained by the response to virus. For example, we have never observed interferon upregulation in pDCs cultured but not stimulated. Moreover, markers upregulated by stimulation in cluster 5 were specifically observed in virus-exposed pDCs by flow cytometry but not in pDCs cultured in the absence of virus. Therefore, the antiviral response likely represents the main driver of separation between cluster 0 and the remaining pDC clusters. Future experiments with finer timeseries may be amenable to pseudotime analyses detailing the transcriptional evolution of pDCs from baseline to phenotypic divergence.

In summary, we have applied novel techniques to the study of pDC function and identity. Our results shed new light on pDC secretory activity at baseline and upon stimulation. Altogether, these findings suggest a need to address new aspects of pDC biology, which do not necessarily center on cell activation or IFN-I secretion. Furthermore, the pDC maturation trajectories described here bear clinical relevance in terms of use as biomarkers for disease states, towards pDC-centric immunotherapies and towards TLR7/9-based vaccine adjuvants.

MATERIALS AND METHODS

pDC Isolation and Culture

For the secretome experiments, pDCs were enriched from leukopaks obtained from the New York Blood Center. First, PBMCs were extracted over Ficoll, and then, pDCs were enriched using EasySep Human Plasmacytoid DC Enrichment Kit [Cat # 19062]. pDCs were cultured in a 1:1 mixture of Advanced RPMI-1640 [Gibco 12633012] and RPMI-1640 [Gibco 11875119], without serum supplementation in ultra-low protein binding 24-well plates. Where indicated, influenza virus H1N1 A/PR/8/34 [Advanced Biotechnologies] at 0.4 HAU/mL was used for stimulation.

For pDC scRNA-seq, human donors were recruited from the Genotype and Phenotype Registry [GaP], a living biobank of genotyped individuals who have volunteered for recall on the basis of their genotype (33). GaP donors are genotyped on the Illumina Global Screening Array (GSA). Demographic data on the GaP donors can be found in **Table S4**. 100CC fresh whole blood was drawn from these donors into sodium-heparin vacutainers. PBMCs were extracted over Ficoll. pDCs were isolated from PBMCs using Miltenyi Plasmacytoid Dendritic Cell Isolation Kit II, human [Cat# 130-092-207]. pDC purity was determined by flow cytometry against BDCA2 and/or BDCA4. pDCs were cultured in Advanced RPMI-1640 [Gibco 12633012]

supplemented with 5% FCS, with the same concentration of influenza virus as in the secretome experiment.

Sample Preparation for Proteomics

Methods are summarized here with additional details described previously (34). Secreted proteins from three biological replicates of each treatment were precipitated with chloroform/methanol, reduced, alkylated, and digested with trypsin. Samples were desalted using Nestgroup C18 Macrospin columns. Eluted peptides were lyophilized, and redissolved in 3% acetonitrile, 0.1% formic acid.

Liquid Chromatography and Mass Spectrometry

Separations were performed with an Ultimate 3000 RSLCNano (Thermo Scientific) and a 75 μ m ID x 50 cm Acclaim PepMap reversed phase C18, 2 μ m particle size column. Flow rate was 300 nL/min with an acetonitrile/formic acid gradient and a column temperature of 40 °C with details as described previously (34).

Mass spectra were collected with a Q Exactive HF mass spectrometer (Thermo Scientific) in positive ion mode using data-dependent acquisition (DDA). Settings included top 15, resolution 120,000 for MS, 15,000 for MS/MS, dynamic exclusion for 20 s and maximum injection time 30 ms for MS and 100 ms for MS/MS. NCE was 28.0, source 2.2kV and 250 °C and S-Lens RF at 55%.

Data processing was done with Elucidator software (Protein Expression Data Analysis System (Ver. 4.0.0.2.31, Ceiba Solutions/PerkinElmer) for label-free quantitation based on comparison of MS1 feature volume. PeptideTeller was set to 0.01 predicted error. Protein identifications were obtained by searching against a database from UniProtKB Release 2020_01, 26-Feb-2020 with 43,392 sequences using Mascot server V. 2.5.1. The database included human reference proteome UP000005640 of reviewed canonical sequences with isoforms as well as the Influenza A virus (strain A/Puerto Rico/8/1934 H1N1) reference proteome UP000170967 with 25 sequences. Also included were porcine trypsin, bovine serum albumin, sheep keratin and other standard contaminants. Expression ratios reported were calculated by the software at the peptide level rather the protein level.

All mass spectrometry raw files are deposited in at the MassIVE public repository (<https://massive.ucsd.edu/>) under accession number MSV000088375.

Single Cell RNA-Seq

For the scRNA-seq experiments, isolated pDCs were cultured in Advanced RPMI-1640 [Gibco 12633012] supplemented with 5% FCS, with the same concentration of influenza virus as in the secretome experiment where indicated. pDCs were counted, pooled at equal ratios from the 3 donors for each time condition, washed, resuspended in PBS/0.4% BSA at a final concentration of 1000 cells/ul and loaded onto the 10X Chromium Controller (10X Genomics). GEMs (Gel Bead-in Emulsion) were generated using Chromium Next GEM Single Cell 3' GEM, Library & Gel Bead Kit v3.1, following the manufacturer's recommendations. Single cell libraries were

assessed and quantitated using a High Sensitivity DNA chip (Agilent). Libraries were loaded onto a High Output Cartridge v2 (PN # 15057931) at 1.8pM and run on a NextSeq 500 sequencer (Illumina). The raw data from the sequencer was demultiplexed into reads along with cell and unique molecular identified [UMI] barcodes which were then aligned to GrCH38 human reference and quantified *via* CellRangerV3 from 10x Genomics. For each condition, cells belonging to each donor were determined using their genotypes from the GSA and Demuxlet (11). Further downstream analysis was done using Seurat (13). Doublets and ambiguous cells identified by Demuxlet were removed along with any cell with < 200 unique genes, any cell expressing > 20% mitochondrial genes and any gene not identified in at least 3 cells. Clusters were identified using Seurat's SCT transform analysis using 30 PCs with time point as an effect being removed using Harmony (12). Statistical analysis and figure plotting was also done using R [<https://www.r-project.org/>] and Tidyverse (35).

Cytokine ELISAs and Flow Cytometry

Where indicated, IFN- α was quantified from culture media using a pan-subtype ELISA (MABTECH 3425-1H-6).

Intracellular staining for IFN- α 2 was accomplished using BD Cytotfix/Cytoperm in accordance with the manufacturer's protocol, along with a monoclonal anti-IFN antibody (Abcam EPR19074). LILRB2 (564345), BDCA4 (565951) and BDCA2 (566427) antibodies were obtained from BD. Cells were acquired on the BD Fortessa flow cytometer and data were analyzed using FlowJo v10.

DATA AVAILABILITY STATEMENT

The datasets presented in this study can be found in online repositories. The names of the repository/repositories and accession number(s) can be found below: <https://www.ncbi.nlm.nih.gov/geo/query/acc.cgi?acc=GSE189120> (sequencing data), <https://massive.ucsd.edu/ProteoSAFe/dataset.jsp?task=4bf41f6d82a49afbbec8f1614a2a171> (proteomic data).

ETHICS STATEMENT

The studies involving human participants were reviewed and approved by Institutional Review Board and Committee for

Participant Protection at the Feinstein Institutes for Medical Research/Northwell Health. The patients/participants provided their written informed consent to participate in this study.

AUTHOR CONTRIBUTIONS

MG and PG conceived the study. MG, KS, LB, and PG designed the experiments. MG, HK, EW, and JC performed the experiments. MG, AS, EW, JC, LB, KS, and PG analyzed the data. MG, AS, KS, LB, and PG wrote the paper. All authors reviewed and approved the final manuscript.

ACKNOWLEDGMENTS

We thank our blood donors for their contribution to this work. Gila Klein, Margaret DeFranco, Kristine Elmaliki and Dorean Flores coordinated GaP donor recall and blood draws. Drs. Sun Jung Kim, Betsy Barnes and Patricia Fitzgerald-Bocarsly provided helpful discussions. Christopher Colon and Barrett Waling assisted with flow cytometry. We appreciate help from Shahar Goeta for technical support with the proteomics work. LB gratefully acknowledge the funding support from NYSTEM contract C029159 for the mass spectrometer (New York State Stem Cell Science Board, LB). Matching funds (LB) from Columbia University through the Department of Biological Sciences, Dean of Science, Executive Vice President for Arts and Sciences, Executive Vice President for Research, Department of Biomedical Engineering, Department of Medicine, the Fu Foundation School Engineering & Applied Science and the Columbia Stem Cell Initiative are also appreciated. We thank Davey Liu for uploading the mass spectrometry data to a public archive. This paper is dedicated in memory of Andrey Y. Bondarenko (1968 - 2019), the developer and architect of the Rosetta Elucidator software, who helped our team learn and perform proteomic data analysis.

SUPPLEMENTARY MATERIAL

The Supplementary Material for this article can be found online at: <https://www.frontiersin.org/articles/10.3389/fimmu.2022.814627/full#supplementary-material>

REFERENCES

- Lennert K, Remmele W. Karyometrische Untersuchungen an Lymphknoten zellen Des Menschen. *Acta Haematol* (1958) 19:99–113. doi: 10.1159/000205419
- Siegal FP, Kadowaki N, Shodell M, Fitzgerald-Bocarsly PA, Shah K, Ho S, et al. The Nature of the Principal Type 1 Interferon-Producing Cells in Human Blood. *Science* (1999) 284:1835–7. doi: 10.1126/science.284.5421.1835
- Baechler EC, Batliwalla FM, Karypis G, Gaffney PM, Ortmann WA, Espe KJ, et al. Interferon-Inducible Gene Expression Signature in Peripheral Blood Cells of Patients With Severe Lupus. *Proc Natl Acad Sci* (2003) 100:2610–5. doi: 10.1073/pnas.0337679100
- Crow MK, Ronnblom L. Type I Interferons in Host Defence and Inflammatory Diseases. *Lupus Sci Med* (2019) 6:e000336. doi: 10.1136/lupus-2019-000336
- Deal EM, Lahl K, Narváez CF, Butcher EC, Greenberg HB. Plasmacytoid Dendritic Cells Promote Rotavirus-Induced Human and Murine B Cell Responses. *J Clin Invest* (2013) 123:2464–74. doi: 10.1172/JCI60945
- Psarras A, Antanaviciute A, Alase A, Carr I, Wittmann M, Emery P, et al. TNF- α Regulates Human Plasmacytoid Dendritic Cells by Suppressing IFN-

- α Production and Enhancing T Cell Activation. *J Immunol* (2021) 206:785–96. doi: 10.4049/jimmunol.1901358
7. Smith N, Rodero MP, Bekaddour N, Bondet V, Ruiz-Blanco YB, Harms M, et al. Control of TLR7-Mediated Type I IFN Signaling in pDCs Through CXCR4 Engagement—A New Target for Lupus Treatment. *Sci Adv* (2019) 5. doi: 10.1126/sciadv.aav9019
 8. Polson C, Sarkar P, Inclendon B, Raguvaran V, Grant R. Optimization of Protein Precipitation Based Upon Effectiveness of Protein Removal and Ionization Effect in Liquid Chromatography–Tandem Mass Spectrometry. *J Chromatogr B* (2003) 785:263–75. doi: 10.1016/S1570-0232(02)00914-5
 9. Thomas JM, Pos Z, Reinboth J, Wang RY, Wang E, Frank GM, et al. Differential Responses of Plasmacytoid Dendritic Cells to Influenza Virus and Distinct Viral Pathogens. *J Virol* (2014) 88:10758–66. doi: 10.1128/JVI.01501-14
 10. Thul PJ, Akesson L, Wiking M, Mahdessian D, Geladaki A, Ait Blal H, et al. A Subcellular Map of the Human Proteome. *Science* (2017) 356. doi: 10.1126/science.aal3321
 11. Kang HM, Subramaniam M, Targ S, Nguyen M, Maliskova L, McCarthy E, et al. Multiplexed Droplet Single-Cell RNA-Sequencing Using Natural Genetic Variation. *Nat Biotechnol* (2017) 36:89–94. doi: 10.1038/nbt.4042
 12. Korsunsky I, Millard N, Fan J, Slowikowski K, Zhang F, Wei K, et al. Fast, Sensitive and Accurate Integration of Single-Cell Data With Harmony. *Nat Methods* (2019) 16:1289–96. doi: 10.1038/s41592-019-0619-0
 13. Stuart T, Butler A, Hoffman P, Hafemeister C, Papalexi E, Mauck WM, et al. Comprehensive Integration of Single-Cell Data. *Cell* (2019) 177:1888–1902.e1821. doi: 10.1016/j.cell.2019.05.031
 14. Villani AC, Satija R, Reynolds G, Sarkizova S, Shekhar K, Fletcher J, et al. Single-Cell RNA-Seq Reveals New Types of Human Blood Dendritic Cells, Monocytes, and Progenitors. *Science* (2017) 356. doi: 10.1126/science.aah4573
 15. Cisse B, Caton ML, Lehner M, Maeda T, Scheu S, Locksley R, et al. Transcription Factor E2-2 is an Essential and Specific Regulator of Plasmacytoid Dendritic Cell Development. *Cell* (2008) 135:37–48. doi: 10.1016/j.cell.2008.09.016
 16. Ghosh HS, Cisse B, Bunin A, Lewis KL, Reizis B. Continuous Expression of the Transcription Factor E2-2 Maintains the Cell Fate of Mature Plasmacytoid Dendritic Cells. *Immunity* (2010) 33:905–16. doi: 10.1016/j.immuni.2010.11.023
 17. Decalf J, Fernandes S, Longman R, Ahloulay M, Audat F, Lefrerre F, et al. Plasmacytoid Dendritic Cells Initiate a Complex Chemokine and Cytokine Network and are a Viable Drug Target in Chronic HCV Patients. *J Exp Med* (2007) 204:2423–37. doi: 10.1084/jem.20070814
 18. Gundacker NC, Haudek VJ, Wimmer H, Slany A, Griss J, Bochkov V, et al. Cytoplasmic Proteome and Secretome Profiles of Differently Stimulated Human Dendritic Cells. *J Proteome Res* (2009) 8:2799–811. doi: 10.1021/pr8011039
 19. Shimura C, Satoh T, Igawa K, Aritake K, Urade Y, Nakamura M, et al. Dendritic Cells Express Hematopoietic Prostaglandin D Synthase and Function as a Source of Prostaglandin D2 in the Skin. *Am J Pathol* (2010) 176:227–37. doi: 10.2353/ajpath.2010.090111
 20. Chowdhury D, Lieberman J. Death by a Thousand Cuts: Granzyme Pathways of Programmed Cell Death. *Annu Rev Immunol* (2008) 26:389–420. doi: 10.1146/annurev.immunol.26.021607.090404
 21. Assil S, Coleon S, Dong C, Decembre E, Sherry L, Allatif O, et al. Plasmacytoid Dendritic Cells and Infected Cells Form an Interferogenic Synapse Required for Antiviral Responses. *Cell Host Microbe* (2019) 25:730–745 e736. doi: 10.1016/j.chom.2019.03.005
 22. Matsui T, Connolly JE, Michnevitz M, Chaussabel D, Yu CI, Glaser C, et al. CD2 Distinguishes Two Subsets of Human Plasmacytoid Dendritic Cells With Distinct Phenotype and Functions. *J Immunol* (2009) 182:6815–23. doi: 10.4049/jimmunol.0802008
 23. Zhang H, Gregorio JD, Iwahori T, Zhang X, Choi O, Tolentino LL, et al. A Distinct Subset of Plasmacytoid Dendritic Cells Induces Activation and Differentiation of B and T Lymphocytes. *Proc Natl Acad Sci USA* (2017) 114:1988–93. doi: 10.1073/pnas.1610630114
 24. Alculumbre SG, Saint-Andre V, Di Domizio J, Vargas P, Sirven P, Bost P, et al. Diversification of Human Plasmacytoid Predendritic Cells in Response to a Single Stimulus. *Nat Immunol* (2018) 19:63–75. doi: 10.1038/s41590-017-0012-z
 25. Onodi F, Bonnet-Madin L, Meertens L, Karpf L, Poirot J, Zhang SY, et al. SARS-CoV-2 Induces Human Plasmacytoid Predendritic Cell Diversification via UNC93B and IRAK4. *J Exp Med* (2021) 218. doi: 10.1084/jem.20201387
 26. Yun TJ, Igarashi S, Zhao H, Perez OA, Pereira MR, Zorn E, et al. Human Plasmacytoid Dendritic Cells Mount a Distinct Antiviral Response to Virus-Infected Cells. *Sci Immunol* (2021) 6. doi: 10.1126/sciimmunol.abc7302
 27. Cederblad B, Blomberg S, Vallin H, Perers A, Alm GV, Rönnblom L. Patients With Systemic Lupus Erythematosus Have Reduced Numbers of Circulating Natural Interferon- α -Producing Cells. *J Autoimmun* (1998) 11:465–70. doi: 10.1006/jaut.1998.0215
 28. Hancharou AY, Chyzh KA, Titov LP, Soroka NF, DuBuske LM. Characterization Of Plasmacytoid Dendritic Cells From Blood Of Patients With Systemic Lupus Erythematosus. *J Allergy Clin Immunol* (2012) 129. doi: 10.1016/j.jaci.2011.12.374
 29. Peruzzi B, Bencini S, Capone M, Mazzoni A, Maggi L, Salvati L, et al. Quantitative and Qualitative Alterations of Circulating Myeloid Cells and Plasmacytoid DC in SARS-CoV-2 Infection. *Immunology* (2020) 161:345–53. doi: 10.1111/imm.13254
 30. Wilk AJ, Rustagi A, Zhao NQ, Roque J, Martinez-Colon GJ, McKechnie JL, et al. A Single-Cell Atlas of the Peripheral Immune Response in Patients With Severe COVID-19. *Nat Med* (2020) 26:1070–6. doi: 10.1038/s41591-020-0944-y
 31. Ren X, Wen W, Fan X, Hou W, Su B, Cai P, et al. COVID-19 Immune Features Revealed by a Large-Scale Single-Cell Transcriptome Atlas. *Cell* (2021) 184:1895–1913.e1819. doi: 10.1016%2Fj.cell.2021.01.053
 32. Chua RL, Lukassen S, Trump S, Hennig BP, Wendisch D, Pott F, et al. COVID-19 Severity Correlates With Airway Epithelium-Immune Cell Interactions Identified by Single-Cell Analysis. *Nat Biotechnol* (2020) 38:970–9. doi: 10.1038/s41587-020-0602-4
 33. Gregersen PK, Klein G, Keogh M, Kern M, DeFranco M, Simpfendorfer KR, et al. The Genotype and Phenotype (GaP) Registry: A Living Biobank for the Analysis of Quantitative Traits. *Immunol Res* (2015) 63:107–12. doi: 10.1007/s12026-015-8711-8
 34. Wobma HM, Tamargo MA, Goeta S, Brown LM, Duran-Struuck R, Vunjak-Novakovic G. The Influence of Hypoxia and IFN- γ on the Proteome and Metabolome of Therapeutic Mesenchymal Stem Cells. *Biomaterials* (2018) 167:226–34. doi: 10.1016/j.biomaterials.2018.03.027
 35. Wickham H, Averick M, Bryan J, Chang W, McGowan LD'A, François R, et al. Welcome to the Tidyverse. *J Open Source Softw* (2019) 4:1686. doi: 10.21105/joss.01686

Conflict of Interest: The authors declare that the research was conducted in the absence of any commercial or financial relationships that could be construed as a potential conflict of interest.

Publisher's Note: All claims expressed in this article are solely those of the authors and do not necessarily represent those of their affiliated organizations, or those of the publisher, the editors and the reviewers. Any product that may be evaluated in this article, or claim that may be made by its manufacturer, is not guaranteed or endorsed by the publisher.

Copyright © 2022 Ghanem, Shih, Khalili, Werth, Chakrabarty, Brown, Simpfendorfer and Gregersen. This is an open-access article distributed under the terms of the Creative Commons Attribution License (CC BY). The use, distribution or reproduction in other forums is permitted, provided the original author(s) and the copyright owner(s) are credited and that the original publication in this journal is cited, in accordance with accepted academic practice. No use, distribution or reproduction is permitted which does not comply with these terms.